

# Journal of Biomedical Optics

BiomedicalOptics.SPIEDigitalLibrary.org

## Femtosecond laser surgery of two-cell mouse embryos: effect on viability, development, and tetraploidization

Alina A. Osychenko  
Alexandr D. Zalessky  
Andrey N. Kostrov  
Anastasia V. Ryabova  
Alexander S. Krivokharchenko  
Viktor A. Nadtochenko

**SPIE.**

Alina A. Osychenko, Alexandr D. Zalessky, Andrey N. Kostrov, Anastasia V. Ryabova, Alexander S. Krivokharchenko, Viktor A. Nadtochenko, "Femtosecond laser surgery of two-cell mouse embryos: effect on viability, development, and tetraploidization," *J. Biomed. Opt.* **22**(12), 125006 (2017), doi: 10.1117/1.JBO.22.12.125006.

# Femtosecond laser surgery of two-cell mouse embryos: effect on viability, development, and tetraploidization

Alina A. Osychenko,<sup>a,\*</sup> Alexandr D. Zalessky,<sup>a,b</sup> Andrey N. Kostrov,<sup>a</sup> Anastasia V. Ryabova,<sup>c,d</sup> Alexander S. Krivokharchenko,<sup>a</sup> and Viktor A. Nadochenko<sup>a,e,f</sup>

<sup>a</sup>Russian Academy of Sciences, N.N. Semenov Institute of Chemical Physics, Moscow, Russia

<sup>b</sup>Moscow Institute of Physics and Technology (State University), Department of Molecular and Biological Physics, Moscow Region, Russia

<sup>c</sup>Prokhorov General Physics Institute Russian Academy of Sciences, Natural Sciences Center, Laser Biospectroscopy Lab, Moscow, Russia

<sup>d</sup>National Research Nuclear University Moscow Engineering Physics Institute, Institute of Engineering Physics for Biomedicine,

Department of Laser Micro and Nano Technologies (87), Moscow, Russia

<sup>e</sup>Institute of Problems of Chemical Physics Russian Academy of Sciences, Department of Structure of Matter, Chernogolovka, Moscow Region, Russia

<sup>f</sup>Moscow State University, Faculty of Chemistry, Moscow, Russia

**Abstract.** The effect of the laser pulse energy and total expose of the energy incident on the embryo blastomere fusion probability was investigated. The probability of the four different events after laser pulse was determined: the fusion of two blastomeres with the following formation of tetraploid embryo, the destruction of the first blastomere occurs, the second blastomere conservation remains intact, the destruction and the death of both cells; two blastomeres were not fused, and no morphological changes occurred. We report on viability and quality of the embryo after laser surgery as a function of the laser energy incident. To characterize embryo quality, the probability of the blastocyst stage achievement was estimated and the blastocyst cells number was calculated. Blastocoel formation is the only event of morphogenesis in the preimplantation development of mammals, so we assumed it as an indicator of the time of embryonic “clocks” and observed it among fused and control embryos. The blastocoel formation time is the same for fused and control embryos. It indicates that embryo clocks were not affected due to blastomere fusion. Thus, the analysis of the fluorescence microscopic images of nuclei in the fused embryo revealed that nuclei fusion does not occur after blastomere fusion. © 2017 Society of Photo-Optical Instrumentation Engineers (SPIE) [DOI: 10.1117/1.JBO.22.12.125006]

Keywords: cell fusion; femtosecond laser; gas–vapor bubble; laser toxicity; tetraploid embryo.

Paper 170280RR received May 10, 2017; accepted for publication Nov. 21, 2017; published online Dec. 20, 2017.

## 1 Introduction

Artificial cell fusion is a topical direction in biology, which opens wide opportunities for fundamental research and biotechnological development. The technology of cell fusion is used to obtain hybridomas<sup>1</sup> in terms of reprogramming and transforming the cell pathway, as well as for gene transfer and genetic therapy.<sup>2</sup> Moreover, laser nanosurgery approach can be successfully used to perform reproductive and therapeutic cloning,<sup>3,4</sup> including the tetraploid embryo application.<sup>5</sup>

Femtosecond cell fusion is one of the innovative techniques, which can be applied to tetraploid embryo production by means of blastomere fusion. Nowadays, a number of classical methods, such as inhibition of cell cleavage using colchicine<sup>6</sup> or cytochalasin B,<sup>7</sup> blastomere fusion using Sendai virus,<sup>8,9</sup> fusion by polyethylene glycol,<sup>10–12</sup> and electrofusion,<sup>13–18</sup> have demonstrated the possibility of tetraploid embryo production. It is quite important to underline that cell fusion under the action of femtosecond laser has a significant advantage over other methods: laser impact disturbs extremely small volume into focal area (about several femtoliters). Absorption of laser irradiation practically does not occur outside focal volume, providing minimal

invasiveness of laser impact.<sup>19,20</sup> Moreover, only laser nanosurgery allows fusing of selected blastomeres into multicellular embryo (fusing 2 or 3 blastomeres in four-cell embryo) without affecting the whole embryo.<sup>21</sup>

In addition to laser-induced intraembryonic blastomere fusion, the effect of femtosecond laser irradiation on embryo viability can be of great interest for science. It was demonstrated that fused embryo viability after pico- and femtosecond-laser treatment remains relatively high compared with control untreated group.<sup>21–23</sup> At this time, there is a number of works<sup>13–18,21,22,24</sup> considered to the blastomere fusion technique. As far as you can see, all these investigations pay attention only to fused (tetraploid) embryo development. Nevertheless, the research of not fused or partly destroyed embryo viability and development after femtosecond laser treatment still was not carried out. Not fused embryo group studying allows determination of the effect of the laser impact by itself. Thus, for example, not fused embryos after electrofusion stop their development. That is why the main problem of this study was to reveal the effect of tightly focused femtosecond-laser impact on certain biological events in the mouse embryos development.

Actually, highly localized laser disruption inside biological media, which can be transparent for near infrared (IR) radiation

\*Address all correspondence to: Alina A. Osychenko, E-mail: [alina.chemphys@gmail.com](mailto:alina.chemphys@gmail.com)

at low irradiance, might be achieved by means of using femtosecond pulses focused on the objective of high numerical aperture.<sup>25–29</sup> So, this fine subdiffraction (with limited resolution of laser influence) is provided by nonlinear absorption of ultra-short laser pulses. Accordingly, nonlinear absorption diminishes the volume in which the laser energy can be deposited. It should be pointed out that the main mechanism of femtosecond nanosurgery is commonly implemented along the path of plasma formation below the optical breakdown threshold.<sup>30,31</sup> However, the explanation of the mechanisms underlying femtosecond-laser nanosurgery of cells and biological tissues in terms of thermal, chemical, and thermomechanical effects should be taken into consideration.

In this paper, first, the answers to the following questions are given: (1) what is the threshold for gas–vapor bubble formation? (2) how does the gas–vapor bubble affect the embryo development and how does the laser irradiation dose affect the probability of blastomere fusion and destruction, as well as embryo viability and quality? (3) what is the tetraploidization mechanism after the femtosecond-laser fusion? and (4) does the femtosecond-laser exposure affect the embryonic “clocks” in fusion, nonfusion, and half-destruction events?

This study deals with the phenomenon of invasiveness of femtosecond-laser exposure that is accurately researched. Experiments were carried out using the femtosecond pulses with a wavelength of 800 nm and 100-fs pulse duration. Additionally, it should be noticed that two-cell mouse embryos were used as a model system. It was shown that gas–vapor bubble formation is necessary, but insufficient for cell fusion. This study exhibits the decrease in the blastocyst formation rate and the blastocyst cell number after gas–vapor generation for the first time. This means that the bubble has a toxic effect for the embryo. Nevertheless, this laser nanosurgery method is an effective method to study blastomere fusion process and fused embryo development in detail. We suppose that tetraploidization occurs due to the mitosis delay rather than the fusion of nuclei or the formation of a common metaphase plate.

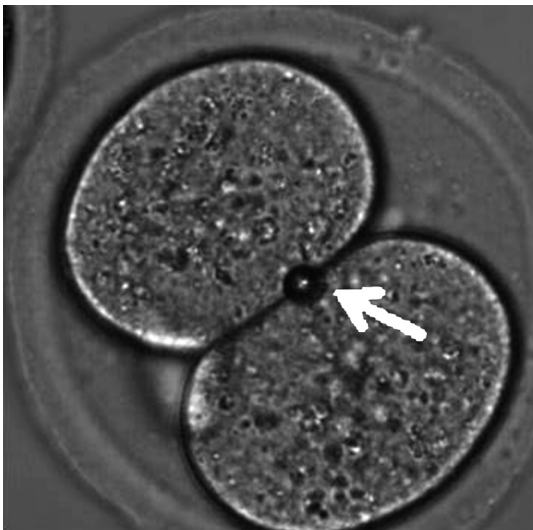


**Fig. 1** The two-cell embryo. An arrow shows gas–vapor bubble in the area of contact produced by femtosecond laser irradiation. Pulse energy was 1 nJ and pulse duration train was 60 ms. The average power was 80 mW and total energy incident was  $2.4 \times 10$  mJ.

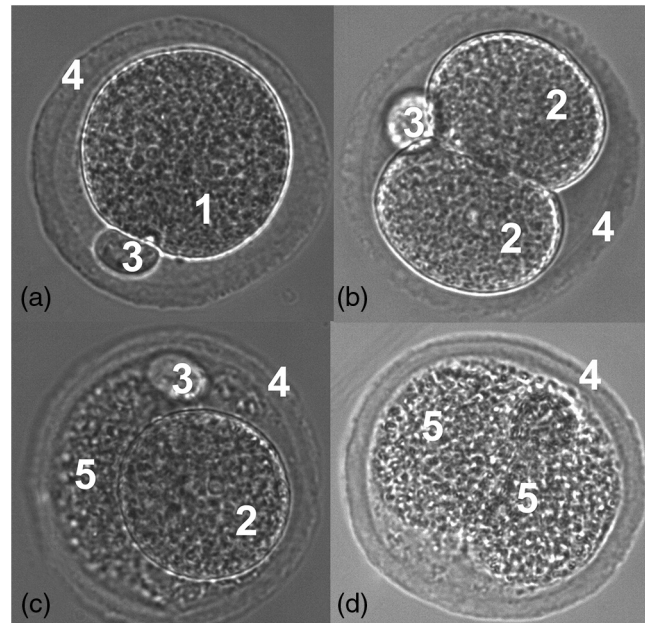


**Fig. 2** Four possible outcomes were realized after laser action: (a) blastomeres were fused, (b) blastomeres were not fused and no morphological changes occurred, (c) one of blastomeres was destroyed, and (d) both blastomeres were destroyed. Images were obtained 2 h later after laser exposure. Structural components of the images are labelled with numbers: 1: fused cell, 2: whole blastomere, 3: polar body, 4: zona pellucida, and 5: destroyed blastomere.

## 2 Results

### 2.1 Embryo Viability, Quality, and Development after Laser Impact

Laser nanosurgical operations were performed using two experimental modes. At the first mode, pulse trains were repeated five times for each sample in different spots of cell contact, so each sample had definite total exposure time. At the second mode, the number of pulse trains was different for each sample. Pulse trains were repeated until a gas–vapor bubble occurred (Fig. 1). At the first mode, the gas–vapor bubble occurred as well but not in every sample.

After the laser action, four possible outcomes obtained (Fig. 2): (a) first, blastomeres were fused, (b) second, blastomeres were not fused, and no morphological changes occurred, (c) third, the one blastomere was destroyed, and (d) finally, both blastomeres were destroyed. Embryo blastomere fusion proceeded about an hour. All embryos, except those, which were completely destroyed, were capable of developing to the blastocyst stage.

#### 2.1.1 Laser impact with different intensities and fixed total exposure time

In this mode, three energy parameters 0.3-, 1-, and 2-nJ pulse were used, which can correspond to 24-, 80-, and 160-mW average power parameters, respectively. Furthermore, three pulse train duration parameters 15, 30, and 60 ms were used. The value of pulse train duration corresponds to the total number of pulses:  $12 \times 10^5$  pulses for 15 ms,  $24 \times 10^5$  for 30 ms, and  $48 \times 10^5$  for 60 ms. All parameters are combined with each other, so, there were nine experimental groups and the one control group. To calculate the total energy incident, multiply the average

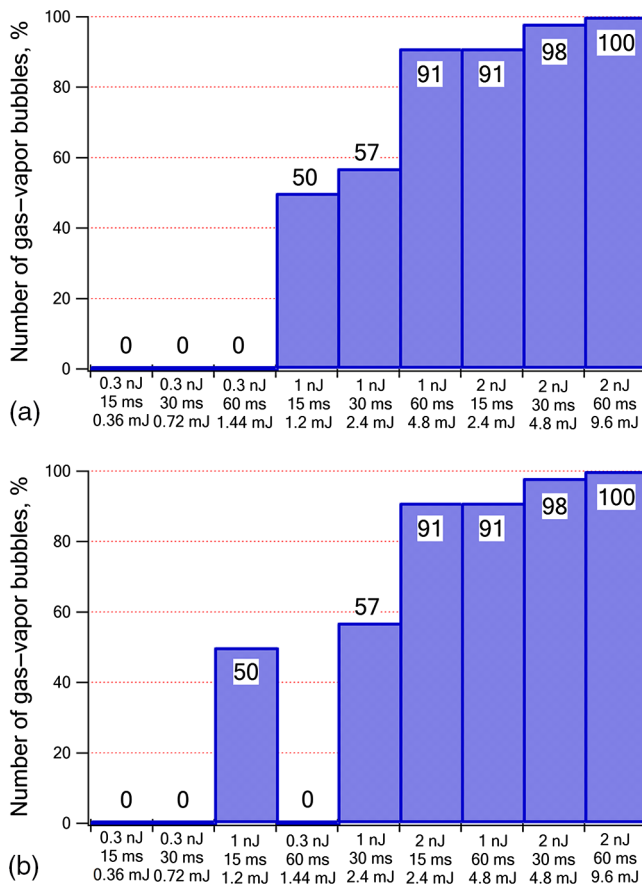


**Fig. 3** Frequency of gas-vapor bubble formation. (a) Probability of vapor-gas bubble formation plotted against increasing the pulse energy and (b) probability of vapor-gas bubble formation plotted against increasing total energy incident.

power by the exposure time, or multiply the pulse energy by the total number of pulses.

With femtosecond 0.3 to 2 nJ pulse energy and 100-fs pulse duration, the peak power density varies from  $2.0 \times 10^{11}$  to  $13.2 \times 10^{11}$  W/cm<sup>2</sup>. The embryo (which is transparent for a wavelength of 800 nm) absorbs  $n$  photons with probability  $p_n = \sigma_n I_n$  ( $n \geq 2$ ,  $\sigma_n$ —absorption cross section for the  $n$ -photon process) at these intensities. So, these conditions are sufficient for the absorption, which can occur apparently. The intensity ( $I$ ) is proportional to the peak power density and also proportional to the pulse energy, which is divided by the pulse duration. As far as the pulse duration is concerned, it remained constant (100 fs) in all the experiments, probability of femtosecond pulse absorption primarily depended on the pulse energy rather than on the average power. This can be seen in the Fig. 3. In Fig. 3(a), the probability of vapor-gas bubble formation is plotted against the pulse energy and corresponding pulse train duration. It is obvious that with increasing pulse energy, the frequency of bubble formation increases as well. A completely different situation is observed in the Fig. 3(b), in which the same data were plotted against the total energy incident. Thus, at the energy value  $12 \times 10^{-4}$  J the probability of the bubble formation is 51%, and at a higher energy  $14.4 \times 10^{-4}$  J it is 0%. Moreover, at the energy equal to  $2.4 \times 10^{-3}$  J the probability of the bubble formation turns out to be 57% and 91%. This ensures us that femtosecond-laser absorption processes have nonlinear nature. Hence, in our case, the average power cannot be a defining

characteristic of femtosecond-laser irradiance. Therefore, the peak power, which is equal to the pulse energy divided by the pulse duration, or pulse energy itself should be taken into account.

The laser beam was focused on the contact area between two blastomeres. The axial position of the laser focal spot was previously adjusted with the painted cover glass. The smallest spot on the cover glass after irradiation was achieved with the image of the glass being in focus. In the experiments, the cell-cell junction between two-cell embryos was moved into the laser focus by adjusting motorized stage and fine focus adjustment knob of the microscope. The femtosecond treatment of the embryos was executed when the cell-cell junction was distinctly detected in the equatorial plane. The impact on the contact area was repeated five times. In some cases, gas-vapor bubble occurred in the irradiation point (Fig. 1). The rate of gas-vapor bubble formation was counted for each parameter (Fig. 3). The mean bubble size and lifetime are also shown in the following Figs. 4(a) and 4(b). Each group had 20 embryos to analyze and statistics of possible outcomes for each group is shown in the Table 1.

The group of interest was presented by not fused embryos. Development and blastocyst cell number of other groups were not studied in this experimental mode. After the laser treatment, not fused embryos were capable of further development to the blastocyst stage (Table 2). On the fifth day, embryos were treated with fluorescence dye Hoechst 33342 for counting cell number by making Z-stack images using confocal imaging (Fig. 5).

Absorption occurs in the focal volume—the area of maximal laser intensity, and it can be resulted into a gas-vapor bubble. Gas-vapor bubble formation is of threshold nature. Threshold was determined as the laser impact parameters that resulted in bubble formation probability exceeding 50%. Within our experiment parameters, the threshold begins to exceed from 1 nJ 15 ms (Fig. 3). With an increase in the pulse duration train within the same pulse energy value, the average bubble lifetime and its size also increased [Figs. 4(a) and 4(b)]. In some cases, where the gas-vapor bubble occurs with a high probability (>90%), the range of the bubble size and lifetime can sharply increase. So, it is clear that lifetime and size of a gas-vapor bubble are proportional to the laser energy absorbed by the embryo.

At low pulse energy (0.3 nJ), embryos did not undergo any morphological changes. At high pulse energy (2 nJ) blastomeres successfully merged, but also the embryos frequently were destroyed. At 1-nJ mode, the number of fused embryos was not high, but the number of destroyed embryos as well was low (Table 1). It should be noticed that cell fusion occurs only in those experimental groups in which the gas-vapor bubble was formed. These results indicate that gas-vapor bubble formation is necessary but insufficient for the cell fusion.

The capability of nonfused embryos to develop to the blastocyst stage (day 5) was not affected by laser treatment within the range of experimental parameters: pulse energy and pulse train duration (Table 2). Statistics was carried out with the exact Fisher test with Bonferroni correction for multiple comparisons. No significant difference was found between experimental and control groups blastocyst rate formation (for each comparison  $P$ -value was  $<0.05/9 = 0.0055$ ). The cell number of these blastocysts was counted. We have found that the blastocyst cell number of treated embryos does not significantly differ from

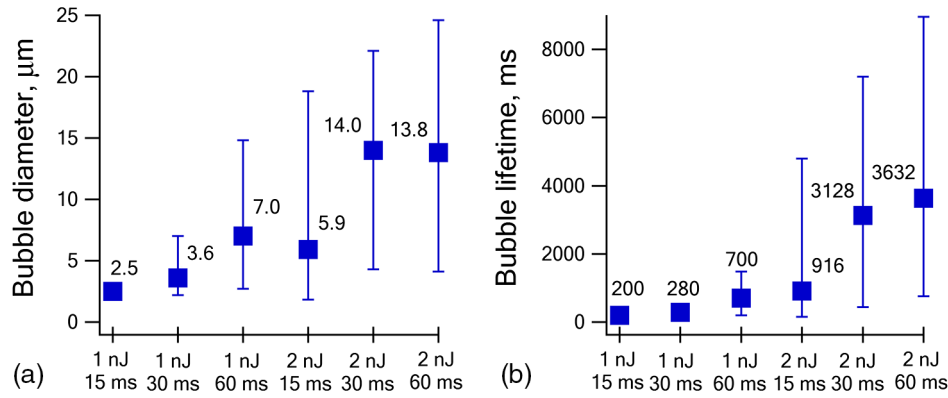


**Fig. 4** (a) The mean gas–vapor bubble size and (b) lifetime. Whiskers show range of values from minimal to maximal. Markers show the mean value of diameter (μm) and lifetime (ms), whiskers show range of values from minimal to maximal.

**Table 1** Outcome’s statistics after laser action with different intensities.

Laser parameters: pulse energy, pulse train duration/total pulse number	Outcome			
	Fused	Not fused	One blastomere destroyed	Completely destroyed embryos
0.3 nJ 15 ms/12 × 10 <sup>5</sup>		20		
0.3 nJ 30 ms/24 × 10 <sup>5</sup>		20		
0.3 nJ 60 ms/48 × 10 <sup>5</sup>		20		
1 nJ 15 ms/12 × 10 <sup>5</sup>	1	19		
1 nJ 30 ms/24 × 10 <sup>5</sup>	5	11	1	3
1 nJ 60 ms/48 × 10 <sup>5</sup>	0	18	1	1
2 nJ 15 ms/12 × 10 <sup>5</sup>	8	10	2	
2 nJ 30 ms/24 × 10 <sup>5</sup>	8	2		10
2 nJ 60 ms/48 × 10 <sup>5</sup>	4	2		14

**Table 2** Not fused embryo development after laser impact. Number of not fused embryos/number of blastocysts originated from not fused embryos; percentage development to the blastocyst stage for the not fused embryos.

Pulse duration train/total number of pulses	Pulse energy		
	0.3 nJ	1 nJ	2 nJ
15 ms/12 × 10 <sup>5</sup>	20/20	12/19	9/10
	100%	63%	90%
30 ms/24 × 10 <sup>5</sup>	20/20	7/11	2/2
	100%	63%	100%
60 ms/48 × 10 <sup>5</sup>	14/20	18/18	1/2
	70%	100%	50%
Control group		24/25	
		96%	

control nontreated group, even for high pulse energy groups (2 nJ 15 ms, 2 nJ 30 ms, and 2 nJ 60 ms).

Variance analysis (ANOVA) with Bonferroni correction for multiple comparisons revealed a significant decrease in the blastocyst cell number only in the 1 nJ 15 ms group ( $p = 0.002$ ) compared with control group. In other groups, significant decrease in blastocyst cell number was not found (Fig. 5).

**2.1.2 Laser impact resulted in gas–vapor bubble formation**

The issue that is dedicated to developmental capability of operated embryos (fused, not fused, embryos with one destroyed blastomere) has been discussed in our previous work.<sup>16</sup> In this part of our research, we observe how laser impact affects the development of all treated embryos in great detail. In this experiment, laser parameters were 1 nJ 30 ms. These parameters were collected from the previous part of this study as they can exceed the gas–vapor bubble formation threshold. The area of contact was irradiated with pulse trains until gas–vapor bubble

formation which was necessary for blastomere fusion (Fig. 1). For this reason, the number of used laser pulse trains differed from one fusion procedure to another.

For 1 nJ 30 ms parameters at this operation mode were received for the following statistics: fusion rate contains 29% (97/330), not fused embryos contain 39% (129/330), one blastomere destroyed—13% (41/330), and completely destroyed blastomeres—19% (64/330).

On day 5, operated and control embryos achieved blastocyst stage, and the percentage of blastocyst achievement is shown in Table 3. Also, the blastocyst cell number was counted on days 5 and 6 (Table 3) to estimate blastocyst quality.

Operated embryos did not develop as successfully to the blastocyst stage as the control ones (Table 3). The exact Fisher test with Bonferroni correction for multiple comparisons has revealed a significant difference between experimental and control groups in the blastocyst stage achievement (for each comparison, the  $P$ -value was  $<0.05/3 = 0.0016$ ).

Also, Table 3 presents data among the blastocyst cell number of operated and control embryos. Cell counting was performed on days 5 and 6 for each group. Both fifth and sixth day

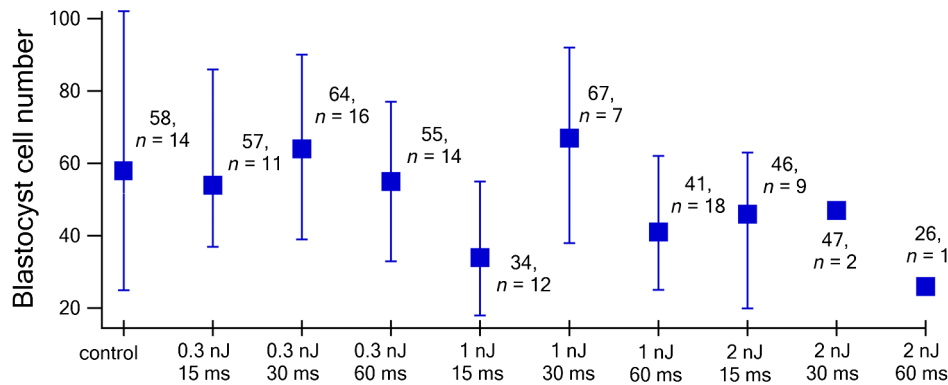


**Fig. 5** Blastocyst cell number of not fused embryos. Markers show the mean number of cells, *n*—number of samples, whiskers show range of values from minimal to maximal.

**Table 3** Development to the blastocyst stage of operated embryos: the percentage of blastocysts and mean the blastocyst cell number at the days 5 and 6.

	Fused embryos	Not fused embryos	Embryos with 1 destroyed blastomere	Control
Number of blastocysts, % (number of blastocysts/total)	49% (47/97)	59% (76/129)	39% (16/41)	84% (131/156)
Mean blastocyst cell number ± standard derivation (number of counted samples), day 5	19 ± 5 ( <i>n</i> = 17)	35 ± 10 ( <i>n</i> = 16)	15 ± 3 ( <i>n</i> = 7)	52 ± 16 ( <i>n</i> = 15)
Mean blastocyst cell number ± standard derivation (number of counted samples), day 6	22 ± 10 ( <i>n</i> = 6)	39 ± 15 ( <i>n</i> = 8)	25 ± 11 ( <i>n</i> = 2)	66 ± 17 ( <i>n</i> = 17)

blastocyst cell number of control embryos is more than the cell number of experimental embryos. This is confirmed by variance analysis (ANOVA) with Bonferroni correction for multiple comparisons: *P*-value for each comparison to control group (fused/control; not fused/control; embryos with one destroyed blastomere/control) was  $<0.05/3 = 0.0016$ . Accordingly, variance analysis (ANOVA) revealed a significant increase in the blastocyst cell number from 5 to 6 days only in control group ( $p = 0.009$ ). There was no significant increase in the blastocyst cell number in other groups. It should be admitted that blastocyst

hatching occurred only in control group and almost not observed in other groups (data not shown). So, this indicates an interruption of the development process.

## 2.2 Fused Embryo Developmental and Morphological Details

Embryo blastomere fusion proceeds about an hour. After blastomere fusion, cell division takes place in 6 to 7 h. It is considered that blastomere’s nuclei fuse in several hours after blastomere

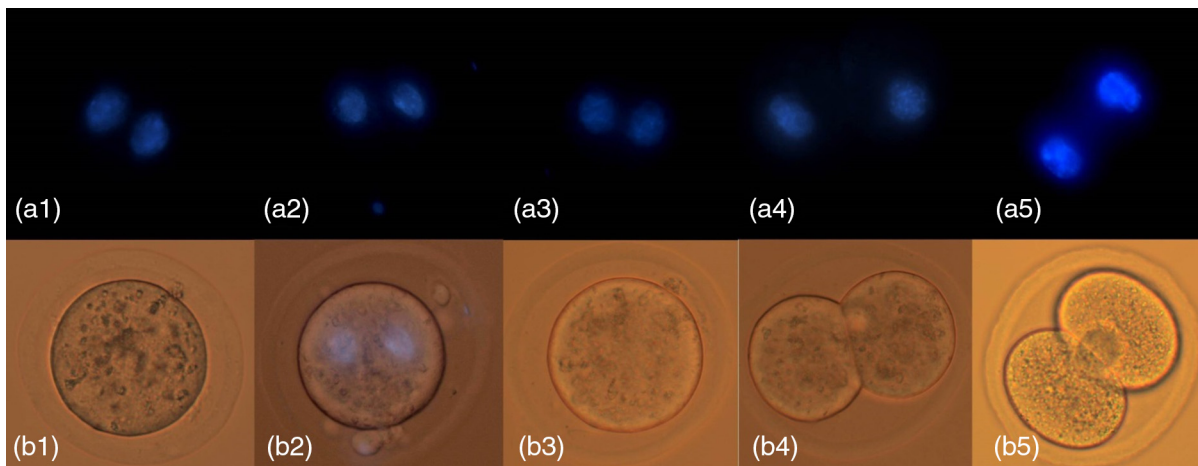


**Fig. 6** Nuclei behavior after femtosecond-laser fusion. (a) Hoechst 33342 fluorescence images, blue color indicates nuclei localization and (b) transmitted light images. 1–4: fused embryos (1 to 2 h after laser fusion; 2 to 4 h after laser fusion; 3 to 6 h after laser fusion; and 4 to 6 h after fusion and immediately after division). 5—control embryo (6 h after other embryos affect).

fusion.<sup>15</sup> According to another data, after the blastomere fusion a common metaphase plate is formed.<sup>12</sup> We studied nuclei behavior in terms of the fusion before the division stage. Every hour one, the fused embryos stained with Hoechst 33342 and was observed by fluorescence and DIC microscopy (Fig. 6). Not only fusion but even convergence was not observed. The nuclei were almost in their places when cytokinesis began. At this point, fused and control embryo nuclei area were equal. We assume that tetraploidization occurs by delaying mitosis and not by fusion of nuclei or the formation of a common metaphase plate.

The process of blastocoel formation—cavitation—occurs during the transition from morula stage to the blastocyst stage. Cavitation was observing when the age of embryos was 92 to 96 h postchorionic gonadotropin injection (day 4 of pregnancy). Compact morula with a cavity is an early blastocyst. Number of early blastocysts and compact morulae was counted. It was found that percentage of early blastocysts does not differ in fused, not fused embryos, and control group (Fig. 7 and Table 4).

The exact Fisher test has not found a significant difference between the ratios of compact morula to early blastocyst for fused, not fused, and control embryos (fused/not fused:  $p = 0.42$ ; fused/control:  $p = 0.60$ ; not fused/control:  $p = 0.85$ , one blastomere destroyed/control:  $p = 0.44$ ). Total early blastocyst percentage is practically equal in fused, not fused, and control groups.

Nuclei area were estimated for diploid (control and not fused) and tetraploid (fused) blastocysts. The mean nucleus area of diploid blastocyst trophoctoderm was  $118 \pm 24 \mu\text{m}^2$  ( $n = 38$ ) for the control group and  $123 \pm 20 \mu\text{m}^2$  ( $n = 38$ ) for the not fused group, and one for tetraploid blastocyst was  $226 \pm 69 \mu\text{m}^2$  ( $n = 38$ ). Tetraploid nucleus area was about two times greater than diploid nucleus (Fig. 8).

Differences in the nuclei area were not observed between control and not fused embryos.

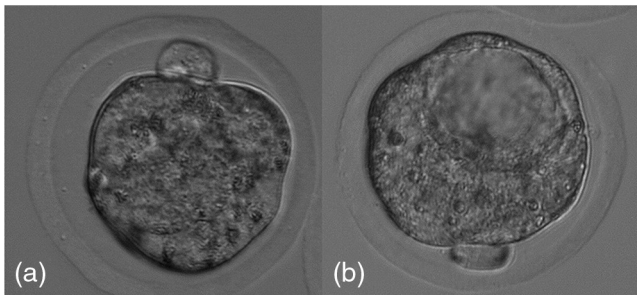


Fig. 7 (a) Compact morula and (b) early blastocyst.

Table 4 Compact morula and early blastocyst ratio in fused, not fused, and control group.

	Fused	Not fused	One blastomere destroyed	Control
Compact morula	30	66	34	102
Early blastocyst	4	15	4	22
Early blastocyst/Total (%)	12	19	11	18

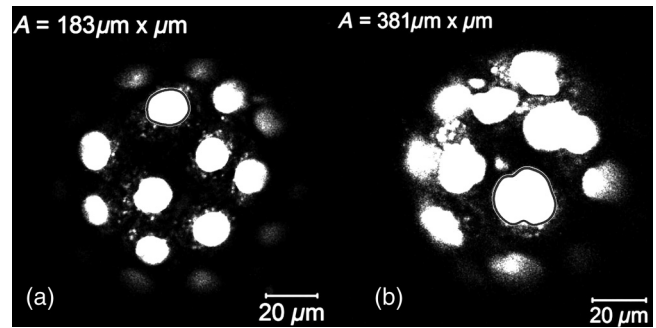


Fig. 8 Blastocyst nuclei area. (a) Control group diploid blastocyst and (b) fused group tetraploid blastocyst.

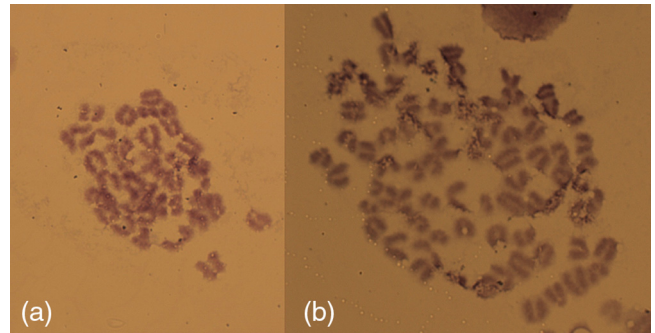


Fig. 9 Karyotype of (a) normal and (b) fused embryos. Blastocysts prepared by Tarkowski air-drying technique<sup>32</sup> stained with Giemsa.

Fused and control embryos were assisted for karyotype at the blastocyst stage using Tarkowski air-drying technique<sup>32</sup> supplemented with colchicine treatment for increasing metaphase plate number. In tetraploid nuclei, there are twice as many chromosomes as in diploid (Fig. 9).

### 3 Discussion

1. In this study, the threshold of gas–vapor bubble formation after the femtosecond-laser irradiation of the two-cell mouse embryo contact area was determined [Fig. 3(a)], and its value was 1 nJ for the 100-fs pulse with 80-MHz repetition rate within parameters studied. With increasing pulse energy, the probability of the gas–vapor bubble formation, its size, and lifetime increases [Figs. 4(a) and 4(b)]. Gas–vapor bubble formation is necessary but insufficient for the cell fusion. Fused embryo development studies<sup>21–23</sup> do not permit separation of the effect of laser impact by itself from the fusion effect. So, the study of not fused (morphologically equal to control) embryo development allows us to understand how the laser impact by itself affects embryo viability and quality.

At the first experimental mode, laser pulse trains were repeated five times for each embryo. First, it turned out that irrespective of the intensity of the impact, the experimental groups developed as successfully as the control one. Embryo destruction occurred within several first hours after laser impact. If the embryo had not been destroyed, it would have developed to the blastocyst stage as well as the control embryo. This conclusion is also confirmed by blastocyst cell counting between

experimental and control groups: no significant difference was found. Apparently, embryo impairment at the initial stage arises through plasmatic membrane integrity damage. Moreover, the effect of viability decreases within investigated parameters and irradiation doze (at later stages) was not found.

At the second experimental mode, laser pulse trains were repeated until the gas–vapor bubble occurred. The parameters 1 nJ 30 ms were used. So, it is obvious that this is the closest above-threshold value and the central value. It was shown that fused and not fused embryos significantly worse develop to the blastocyst stage than the control group embryos. Additionally, there was no significant difference in the percentage of blastocyst formation between fused and not fused embryos.

In accordance, not fused embryo development and blastocyst cell number can allow comparison of the first and the second experimental modes. It was figured out that 63% of not fused embryos developed at the blastocyst stage at the first experimental mode and 59% at the second one. Blastocyst formation rate seems to be equal for both modes. However, blastocyst cell number for these two modes is notably different:  $52 \pm 27$  for the first mode and  $35 \pm 10$  for the second (Fig. 10). Variance analysis (one-way ANOVA) revealed significant difference between these two samples ( $p = 8 \times 10^{-5}$ ).

As far as it is seen, Fig. 10 shows the wide spread of blastocyst cell number in the mode 1, whereas at the mode 2 the spread was not very wide. At the first mode, the bubble formation rate was 57%, so in some embryos bubbles occurred, and in some there were no bubbles. At the second mode, bubble formation rate was 100%, this means that each sample the bubble was formed. The blastocyst cell number decrease at the mode 2 indicates that the gas–vapor bubble has a toxic effect. It is obvious that the development of operated embryos stops on the day 5 (Table 3), which also confirms the gas–vapor bubble toxicity.

Moreover, it is well known that tightly focused femtosecond-laser exposure can result in ionization of the substance and multiphoton chemical bounds dissociation.<sup>33</sup> Formed in this way, radicals, ion-radicals, and solvated electrons are capable to react with oxygen molecules, which eventually lead to the formation of reactive oxygen species, such as superoxide anions, hydroperoxide radicals, and organic peroxy radicals.<sup>20</sup> So, all these peroxy compounds, created in the focal volume, are able to provide toxic effects on the living cell.

It should also be considered that pressure and temperature rise could be produced in the focal volume.<sup>34</sup> Nevertheless, the spreading waves of pressure and temperature shock rapidly

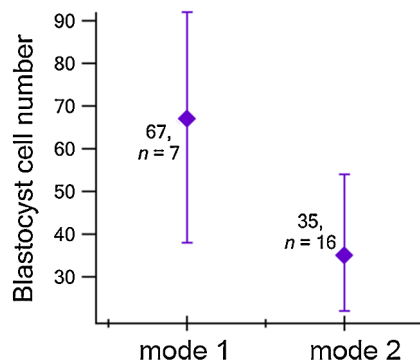


**Fig. 10** Blastocyst cell number in 1 and 2 experimental modes. Laser parameters for both modes were 1 nJ 30 ms. Whiskers show variance of values from minimal to maximal.

decay, it is still able to disturb the cell integrity in the focal area, leading this way to viability decrease.<sup>35</sup>

2. Finally, observation of nuclei behavior after blastomere fusion allowed making a conclusion that nuclei do not fuse after blastomere fusion as it was considered.<sup>22</sup> Tetraploid embryo division occurs without nuclei fusion in 6 h after blastomere fusion. Presumably, tetraploidization has occurred due to essential process of DNA duplication before the second mitosis division. Laser impact causing blastomere fusion delayed the transition from two-celled embryo to four-celled and prevents halving of duplicated DNA in this way. Interestingly, that nuclei size after tetraploidization at the two-cell stage remains equal to diploid nuclei (Fig. 6), but trophoctoderm nuclei have two time greater nuclei size than diploid one (Fig. 8). Thus, air-drying blastocyst preparation proved that fused embryos had tetraploid karyotype (Fig. 9).

It is a fact that the only morphogenesis event in mammalian preimplantation development is cavitation (blastocoel formation). Obviously, cavitation occurs due to ion- and water-transporting proteins activity (Na/K ATPase, AQP9),<sup>36</sup> so the percentage of early blastocyst at the same time of development was not altering in fused, not fused embryos, and control group (Fig. 7 and Table 4).

In conclusion, it should be added that control and not fused embryos are one division ahead of the fused embryos (after laser assisted fusion). Observations were carried out for 48 h after laser exposure and revealed that cavitation has begun with the same probability in all embryo groups: fused, not fused, and control. It is known that transcription and translation for the cavitation process can begin in just a few hours before the blastocoel formation.<sup>37</sup> Thus, our observations suggest that not only laser impact but even blastomere fusion did not affect embryonic clocks of morphogenesis.

## 4 Conclusion

In this research, we investigated the effect of laser dose on embryo viability. It was shown that laser irradiation does not affect embryo viability and quality within the parameters studied. However, the cases of gas–vapor bubble formation decreased embryo developmental capability and blastocyst cell number. Gas–vapor bubble formation is necessary but insufficient for the cell fusion.

Embryo blastomere fusion results in tetraploid embryo formation. We suppose that tetraploidization occurs due to essential process of DNA duplication before the second mitosis division rather than nuclei fusion or common metaphase plate formation. The observation of blastocoel formation showed that neither fusion nor laser exposure by itself affects embryo clocks.

## 5 Materials and Methods

### 5.1 Animals and Embryos

In these experiments, we used C57Bl/6 female mice aged 4 to 8 weeks. C57Bl/6 female mice were superovulated by the standard method of intraperitoneal (i.p.) injection of 10 IU pregnant mare's serum gonadotropin (A036A02, Intervet) followed by an i.p. injection of 10 IU human chorionic gonadotropin (hCG) (A038A01, Intervet) 48 h later. Females were mated overnight

with CBA/C57B16 males and examined following morning for the presence of a vaginal plug (day 1). Two-cell embryos were flushed from the oviducts by M2 medium (M7167, Sigma) 48 h after hCG injection (day 2). The embryos were cultivated in the CO<sub>2</sub> incubator with 5% concentration of the carbon dioxide at the temperature 37°C in the medium M16 (M7292, Sigma) in four-well dishes (179830, Nunc).

All the experiments described in the present work were carried out under the supervision of the Institute of Chemical Physics RAS. Ethics committee approved the experimental protocols.

## 5.2 Experimental Setup

In the experiments, we used the inverted optical Olympus IX71 microscope with the objective 60× and NA = 0.7. Embryo membrane optoperforation was carried out using a femtosecond Mai Tai Ti:sapphire laser (Spectra Physics) generating the radiation at the wavelength 800 nm. The diameter of the beam waist was estimated using the formula for the diffraction limited spot:  $d = 1.22\lambda/\text{NA} = 1.39 \mu\text{m}$ . A series of prisms were used in the setup to compensate for the dispersion of the optical components in the laser path and objective of the microscope. The laser pulse duration was measured directly in the object plane of the microscope using AA-M autocorrelator (Avesta Project) and was determined as 100 fs. The average power was in the range of 24 to 160 mW and the pulse repetition rate was 80 MHz. The estimated power density for the pulse in the beam waist was in the range of 2.0 to  $13.2 \times 10^{11} \text{ W cm}^{-2}$ . The length of the pulse train, controlled with a mechanical shutter (Thorlabs), was from 15 to 60 ms. The visual control was implemented using the CMOS 1.3Mpix Thorlabs camera.

To perform the laser micromanipulations, the embryos were transferred to 24 × 24 mm cover glasses into a drop of the embryonal medium M2 with the volume 50 μL. For fusing two blastomeres, laser pulse was directed to the zone of maximally dense contact between them. The impact was considered as successful if it leads to the formation of a cavitation steam-to-gas bubble.

## 5.3 Confocal Microscopy

The embryos were placed in M16 medium containing 5 mkg/ml Hoechst 33342 (B2261, “Sigma”) staining for 10 to 20 min in CO<sub>2</sub> incubator. Then embryos were flushed in M2 medium and placed in M2 medium drop onto the sterile Petri dish with a glass bottom 0.16-mm-thick. Fluorescence localization was detected using laser scanning confocal microscope LSM-710-NLO (Carl Zeiss Microscopy, Jena, Germany), 20× Plan-Apochromat objective (NA = 0.8). Two-photon excitation of the dye was performed by the 770-nm wavelength laser. Fluorescence recorded at 400/550 nm range. Thereby, the imposition of fluorescence image and images obtained in the transmitted light mode were obtained. 3-D images were received by Z-stack reconstruction. Cell number and nucleus square were counted using ZEN program (Carl Zeiss Microscopy, Jena, Germany).

## 5.4 Estimation of Embryo Karyotype

Fused and control embryos were assessed for karyotype at the blastocyst stage using Tarkowski air-drying technique.<sup>32</sup> Briefly, embryos were preincubated with 0.1 mkg/ml colchicine

(PanEco) during 4 to 5 h to arrest the cleavage division at metaphase. They were then placed in a hypotonic solution of 25% PBS (Sigma) for 30 min at room temperature. Embryos within a microdrop of hypotonic solution were placed on a glass slide and mounted with fixative compound (methyl alcohol:acetic acid = 1:3) and air-dried. These preparations were stained in 7% Giemsa (PanEco) for 15 min.

## 5.5 Statistical Research

Differences between groups were tested for statistical significance using exact Fisher test and variance analysis. Exact Fisher test was calculated online at Ref. 38.

Variance analysis (one-way ANOVA) was carried out using IGOR PRO Ver. 4.0.0.0, serial number 15909. Significant difference for both methods accepted, if *P*-value was lower than 0.05. Bonferroni correction applied for multiple comparisons, so *P*-value calculated: 0.05/number of comparisons.

## Disclosures

The authors have no relevant financial interests in this article and no potential conflicts of interest to disclose.

## Acknowledgments

The work has financial support from the Russian Foundation for basic research in the part of theoretical studies and experimental measurement 16-53-52046 MNT\_a and program BSR 0082-2014-0019.

## References

1. G. Kohler and C. Milstein, “Continuous cultures of fused cells secreting antibody of predefined specificity,” *Nature* **256**(5517), 495–497 (1975).
2. M. Alvarez-Dolado, “Cell fusion: biological perspectives and potential for regenerative medicine,” *Front. Biosci.* **12**, 1–12 (2007).
3. A. K. Shakhbazyan et al., “The use of laser for obtaining recipient cytoplasts for mammalian nuclear transfer,” *Dokl. Biol. Sci.* **428**(3), 475–478 (2009).
4. A. K. Shakhbazyan et al., “The possibilities of optical laser technologies in cell engineering,” *Dokl. Biol. Sci.* **429**(4), 587–590 (2009).
5. D. Wen et al., “Completely ES cell-derived mice produced by tetraploid complementation using inner cell mass (ICM) deficient blastocysts,” *PLoS One* **9**(4), e94730 (2011).
6. R. G. Edwards, “Colchicine-induced heteroploidy in the mouse. II. The induction of tetraploidy and other types of heteroploidy,” *J. Exp. Zool.* **137**(2), 349–362 (1958).
7. M. H. L. Snow, “Tetraploid mouse embryos produced by cytochalasin B during cleavage,” *Nature* **244**, 513–515 (1973).
8. G. T. O’Neill, S. Speirs, and M. H. Kaufman, “Sex-chromosome constitution of postimplantation tetraploid mouse embryos,” *Cytogenet. Cell Genet.* **53**(4), 191–195 (1990).
9. B. S. Song et al., “Inactivated Sendai-virus-mediated fusion improves early development of cloned bovine embryos by avoiding endoplasmic-reticulum-stress-associated apoptosis,” *Reprod. Fertil. Dev.* **23**(6), 826–836 (2011).
10. M. A. Eglitis, “Formation of tetraploid mouse blastocysts following blastomere fusion with polyethylene glycol,” *J. Exp. Zool.* **213**(2), 309–313 (1980).
11. A. Spindle, “Polyethylene glycol-induced fusion of two-cell mouse embryo blastomeres,” *Exp. Cell Res.* **131**(2), 465–470 (1981).
12. G. G. Sekirina et al., “The behavior of mitochondria and cell integration during somatic hybridisation of sister blastomeres of the 2-cell mouse embryo,” *Zygote* **5**, 97–103 (1997).
13. J. Z. Kubiak and A. K. Tarkowski, “Electrofusion of mouse blastomeres,” *Exp. Cell Res.* **157**(2), 561–566 (1985).
14. H. Berg, “Fusion of blastomeres and blastocysts of mouse embryos,” *Bioelectrochem. Bioenerg.* **9**, 223–228 (1982).

15. E. Popova, M. Bader, and A. Krivokharchenko, "Effects of electric field on early preimplantation development in vitro in mice and rats," *Hum. Reprod.* **26**(3), 662–670 (2011).
16. J. P. Ozil and J. A. Modlinski, "Effects of electric field on fusion rate and survival of 2-cell rabbit embryos," *J. Embryol. Exp. Morphol.* **96**, 211–228 (1986).
17. R. S. Prather et al., "Characterization of DNA synthesis during the 2-cell stage and the production of tetraploid chimeric pig embryos," *Mol. Reprod. Dev.* **45**(1), 38–42 (1996).
18. S. Iwasaki et al., "Production of bovine tetraploid embryos by electrofusion and their developmental capability in vitro," *Gamete Res.* **24**(3), 261–267 (1989).
19. K. Kuetemeyer et al., "Repetition rate dependency of low-density plasma effects during femtosecond-laser-based surgery of biological tissue," *Appl. Phys. B Lasers Opt.* **97**(3), 695–699 (2009).
20. A. Vogel et al., "Mechanisms of femtosecond laser nanosurgery of cells and tissues," *Appl. Phys. B Lasers Opt.* **81**(8), 1015–1047 (2005).
21. A. Krivokharchenko et al., "Laser fusion of mouse embryonic cells and intra-embryonic fusion of blastomeres without affecting the embryo integrity," *PLoS One* **7**(12), e50029 (2012).
22. K. Kuetemeyer et al., "Femtosecond laser-induced fusion of nonadherent cells and two-cell porcine embryos," *J. Biomed. Opt.* **16**(8), 088001 (2011).
23. A. V. Karmenyan et al., "Use of picosecond infrared laser for micro-manipulation of early mammalian embryos," *Mol. Reprod. Dev.* **76**(10), 975–983 (2009).
24. A. A. Osychenko et al., "Fusion of blastomeres in mouse embryos under the action of femtosecond laser radiation. Efficiency of blastocyst formation and embryonic development," *Quantum Electron.* **45**(5), 498–502 (2015).
25. Y. R. Shen, *The Principles of Nonlinear Optics*, Wiley, New York (1984).
26. A. Vogel and V. Venugopalan, "Mechanisms of pulsed laser ablation of biological tissues," *Chem. Rev.* **103**, 577–644 (2003).
27. V. Venugopalan et al., "The role of laser-induced plasma formation in pulsed cellular microsurgery and micromanipulation," *Phys. Rev. Lett.* **88**, 078103 (2002).
28. K. König et al., "Intracellular nanosurgery with near infrared femtosecond laser pulses," *Cell. Mol. Biol.* **45**, 195–201 (1999).
29. K. König et al., "Pulse-length dependence of cellular response to intense near-infrared laser pulses in multiphoton microscopes," *Opt. Lett.* **24**(2), 113–115 (1999).
30. A. Vogel, *Optical Breakdown in Water and Ocular Media, and its Use for Intraocular Photodisruption*, Shaker, Aachen (2001).
31. A. Vogel et al., "Femtosecond-laser-produced low-density plasmas in transparent biological media: a tool for the creation of chemical, thermal and thermomechanical effects below the optical breakdown threshold," *Proc. SPIE* **4633**, 23–37 (2002).
32. A. K. Tarkowski, "An air-drying method for chromosome preparations from mouse eggs," *Cytogenesis* **5**, 394–400 (1966).
33. L. V. Keldysh, "Ionization in the field of a strong electromagnetic wave," *J. Exp. Theor. Phys.* **20**(5), 1307–1314 (1965).
34. G. Paltauf and P. E. Dyer, "Photomechanical processes and effects in ablation," *Chem. Rev.* **103**(2), 487–518 (2003).
35. A. Heisterkamp et al., "Pulse energy dependence of subcellular dissection by femtosecond laser pulses," *Opt. Express* **13**(10), 3690–3696 (2005).
36. A. J. Watson, "The cell biology of blastocyst development," *Mol. Reprod. Dev.* **33**(4), 492–504 (1992).
37. G. M. Kidder and J. R. McLachlin, "Timing of transcription and protein synthesis underlying morphogenesis in preimplantation mouse embryos," *Dev. Biol.* **112**(2), 265–275 (1985).
38. <http://www.socscistatistics.com/tests/fisher/Default2.aspx>

**Alina A. Osychenko** is a PhD student and a junior researcher of N. N. Semenov Institute of Chemical Physics, Russian Academy of Sciences (ICP RAS). She graduated from Lomonosov Moscow State University in 2014 and is now preparing her PhD dissertation on biophysics in ICP RAS. Her scientific work deals with the nanosurgery methodic and preimplantation embryo development.

**Alexandr D. Zalessky** graduated from Moscow Institute of Physics and Technology (State University) (MIPT), Department of Molecular and Biological Physics, in 2009 with a specialization in chemical physics. From 2006 to 2007, he did his bachelor research work in the Department of Molecular and Biological Physics, MIPT. He received a master's degree in applied mathematics and physics, ICP RAS in 2009. In 2013, He became a PhD in chemical physics, physics of extreme states of substances.

**Andrey N. Kostrov** graduated from Moscow Institute of Physics and Technology (State University) (MIPT), in 2008 with a specialization in chemical physics. He received a master's degree in applied mathematics and physics, ICP RAS. From 2009 to 2011, he carried out his research work at Laboratoire des Sciences des Procédés et Des Matériaux—CNRS, Université Paris Nord. And in 2011, he became a PhD in chemical physics, physics of extremely states of substance.

**Anastasia V. Ryabova** is a senior researcher of Laser Biospectroscopy Lab in Natural Sciences Center at Prokhorov General Physics Institute Russian Academy of Science. She conducts multidisciplinary studies of phenomena associated with the interaction of light, photosensitizers and biological objects using laser-spectroscopic methods and confocal microscopy. Particular attention is directed to the fluorescence imaging in the NIR range, rare-earth ions doped nanoparticles and crystalline nanoparticles of organic photosensitizers.

**Alexander S. Krivokharchenko** graduated from the Department of Embryology doing a PhD at the Faculty of Biology, Moscow State University, and was awarded a degree in biological sciences. His professional interests are experimental embryology of mammals, *in vitro* manipulations with mammalian gametes and embryos. He is an author and coauthor of about 100 scientific publications and is a reviewer of international medical and scientific journals. He has been a member of a number of international projects.

**Victor A. Nadtochenko** is a director of ICP RAS, Moscow, and a head of the BioNanoStructure Laboratory. He received his MS degree in chemical physics at MIPT in 1976, his PhD in chemical physics at the Institute of Chemical Physics RAS, Moscow, in 1979, and his DrSc in chemistry at the Institute of Problems of Chemical Physics RAS, Chernogolovka, in 2000.